Local Leukocyte Invasion during Hyperacute Human Ischemic Stroke

Alexander M. Kollikowski, MD ,[1]* Michael K. Schuhmann, PhD,[2]*
Bernhard Nieswandt, PhD,[3] Wolfgang Müllges, MD,[2] Guido Stoll, MD,[2] and
Mirko Pham, MD[1]

Objective: Bridging the gap between experimental stroke and patients by ischemic blood probing during the hyperacute stage of vascular occlusion is crucial to assess the role of inflammation in human stroke and for the development of adjunct treatments beyond recanalization.
Methods: We prospectively observed 151 consecutive ischemic stroke patients with embolic large vessel occlusion of the anterior circulation who underwent mechanical thrombectomy. In all these patients, we attempted microcatheter aspiration of 3 different arterial blood samples: (1) within the core of the occluded vascular compartment and controlled by (2) carotid and (3) femoral samples obtained under physiological flow conditions. Subsequent laboratory analyses comprised leukocyte counting and differentiation, platelet counting, and the quantification of 13 proinflammatory human chemokines/cytokines.
Results: Forty patients meeting all clinical, imaging, interventional, and laboratory inclusion criteria could be analyzed, showing that the total number of leukocytes significantly increased under the occlusion condition. This increase was predominantly driven by neutrophils. Significant increases were also apparent for lymphocytes and monocytes, accompanied by locally elevated plasma levels of the T-cell chemoattractant CXCL-11. Finally, we found evidence that short-term clinical outcome (National Institute of Health Stroke Scale at 72 hours) was negatively associated with neutrophil accumulation.
Interpretation: We provide the first direct human evidence that neutrophils, lymphocytes, and monocytes, accompanied by specific chemokine upregulation, accumulate in the ischemic vasculature during hyperacute stroke and may affect outcome. These findings strongly support experimental evidence that immune cells contribute to acute ischemic brain damage and indicate that ischemic inflammation initiates already during vascular occlusion.

Ischemic stroke is the second leading cause of death and disability worldwide.[1] Currently, recanalization by mechanical thrombectomy, in conjunction with intravenous (IV) thrombolysis, if possible, represents the only evidence-based acute treatment for patients with embolic cerebral large-vessel occlusion (LVO; class of recommendation I, level of evidence A).[2] Despite overwhelming treatment effects,[3] serious limitations remain. Among previously functional patients, particularly radiological imaging signs of advanced

or completed irreversible brain infarction and significant delays in presentation or transportation impede eligibility for treatment or impair efficacy.[4–6] Even if provided timely and technically successful, therapeutic recanalization as a prerequisite for stroke recovery alone does not guarantee a favorable outcome.[7–9] This clinically unsatisfactory situation calls for further research regarding the complex and intertwined neurobiological processes of ischemic stroke that lead to final tissue damage.[10]

Experimental data suggest that immune cells and platelets contribute to the evolution of cerebral infarction.[11–15] However, studies in humans are sparse, and data on immune cell accumulation and modulation during the hyperacute stage of ischemic stroke are lacking.[16,17] Animal studies indicate that even after brief episodes of cerebral ischemia, microvascular function is compromised, leading to focal no-reflow despite return of blood flow in the main vascular trunks.[18,19] Histological studies in these animals show very early accumulation of leukocytes and platelets in the microvasculature,[15,19,20] and there is increasing evidence that they functionally contribute to ischemic brain damage.[21–23] To overcome the translational road block with high failure rates in clinical studies of experimentally successful treatments, it is essential to get direct insights into pathophysiological processes in acute stroke patients.[24] With the advent of mechanical thrombectomy, it has become possible and a technically necessary step of this procedure to penetrate into the previously not accessible center of the ischemic circulation by microcatheter navigation. Importantly, during this crucial treatment step, the embolic occlusion persists. Therefore, the ischemic milieu of the arterial compartment distal to the occlusion is uniquely conserved for the sampling of pial arterial blood by microcatheter aspiration. We herein report on this novel approach and show that leukocytes, accompanied by specific chemokine upregulation, strongly accumulate in the human ischemic vasculature distal to the occlusion site and may affect outcome.

Patients and Methods

This study was approved by the local ethics committee (approval # 135/17). All patients or their legal representatives provided written informed consent. Between August 2018 and July 2019, we conducted a prospective observational study in 183 consecutive symptomatic ischemic stroke patients undergoing endovascular thrombectomy to investigate the role of local leukocyte and platelet involvement during the hyperacute stage of LVO of the anterior circulation. The criteria according to which patients had to be excluded from the eligible total cohort of 183 patients were defined a priori and applied to homogenize the target cohort as well as to standardize intraprocedural sample collection, handling, storage, and processing until laboratory analysis. These criteria are described in detail in the paragraphs that follow (Fig 1).

Clinical and imaging inclusion criteria were defined as follows: (1) first-ever ischemic stroke with neurological baseline deficit equivalent to the National Institute of Health Stroke Scale (NIHSS) ≥ 6[25]; (2) multimodal imaging prior to mechanical thrombectomy comprising cranial noncontrast computed tomography (CT; Somatom Definition AS; Siemens Healthcare, Erlangen, Germany), CT-angiography and CT-perfusion scan (complementary) in order (a) to exclude hemorrhage or extensive infarction equivalent to Alberta Stroke Program Early CT Score (ASPECTS) <5, (b) to noninvasively determine the occlusion site, and (c) to confirm patient eligibility in the extended therapeutic time window ≤24 hours, which requires extended imaging according to current guidelines[2]; and (3) periprocedural (invasive angiographic) confirmation of LVO of the following sites: distal internal cerebral artery (ICA-T), middle cerebral artery (MCA) M1 segment, or proximal M2 segment, respectively.

Patients were not included due to the following reasons: (1) proven bilateral or multifocal LVO other than defined; (2) vessel subocclusion (ie, angiographically proven residual or restored antegrade flow); (3) any deviation from the interventional, sampling, and processing protocol (see below); (4) LVO in association with either ≥50% common carotid artery /cervical ICA stenosis or ICA dissection[26]; (5) the requirement of intraprocedural percutaneous transluminal angioplasty (PTA) or stent implantation[27]; and (6) intraprocedural platelet inhibitor use.

We collected the following demographic, clinical, radiological, and interventional data: age, sex, time of symptom onset, baseline medication, baseline heart rate and blood pressure, NIHSS at presentation and at 72 hours, time of noninvasive and angiographic image acquisition, occlusion location, ASPECTS at baseline and at 48 hours, previous intravenous recombinant tissue plasminogen activator (rt-PA) administration, time of blood sampling, and time of recanalization. Leptomeningeal collateral status was graded by CT-angiography in standardized manner using an established 3-point scoring system.[28] Recanalization success was assessed by the modified treatment in cerebral ischemia (mTICI) scale and considered successful for mTICI 2b or mTICI 3.[29] ASPECTS, collateral status, and mTICI were determined by finding a consensus between 2 authors of this study with longstanding experience in stroke imaging, diagnostic cerebral angiography, and vascular neurointervention (A.M.K. and M.P.).

Interventional and Sampling Protocol

The mechanical thrombectomy procedures were performed by board-certified neurointerventional experts or by supervised neurointerventional fellows in a biplane neuroangiography suite (Axiom Artis Q; Siemens Healthcare). All patients were treated under general anesthesia as per institutional standard. Endovascular access for mechanical thrombectomy was obtained by means of a transfemoral approach through the common femoral artery (CFA) using the modified Seldinger technique. Nontherapeutic doses of 1,000IU unfractionated heparin were always added to 1,000ml rinsing fluid (standard 0.9% saline solution) to avoid
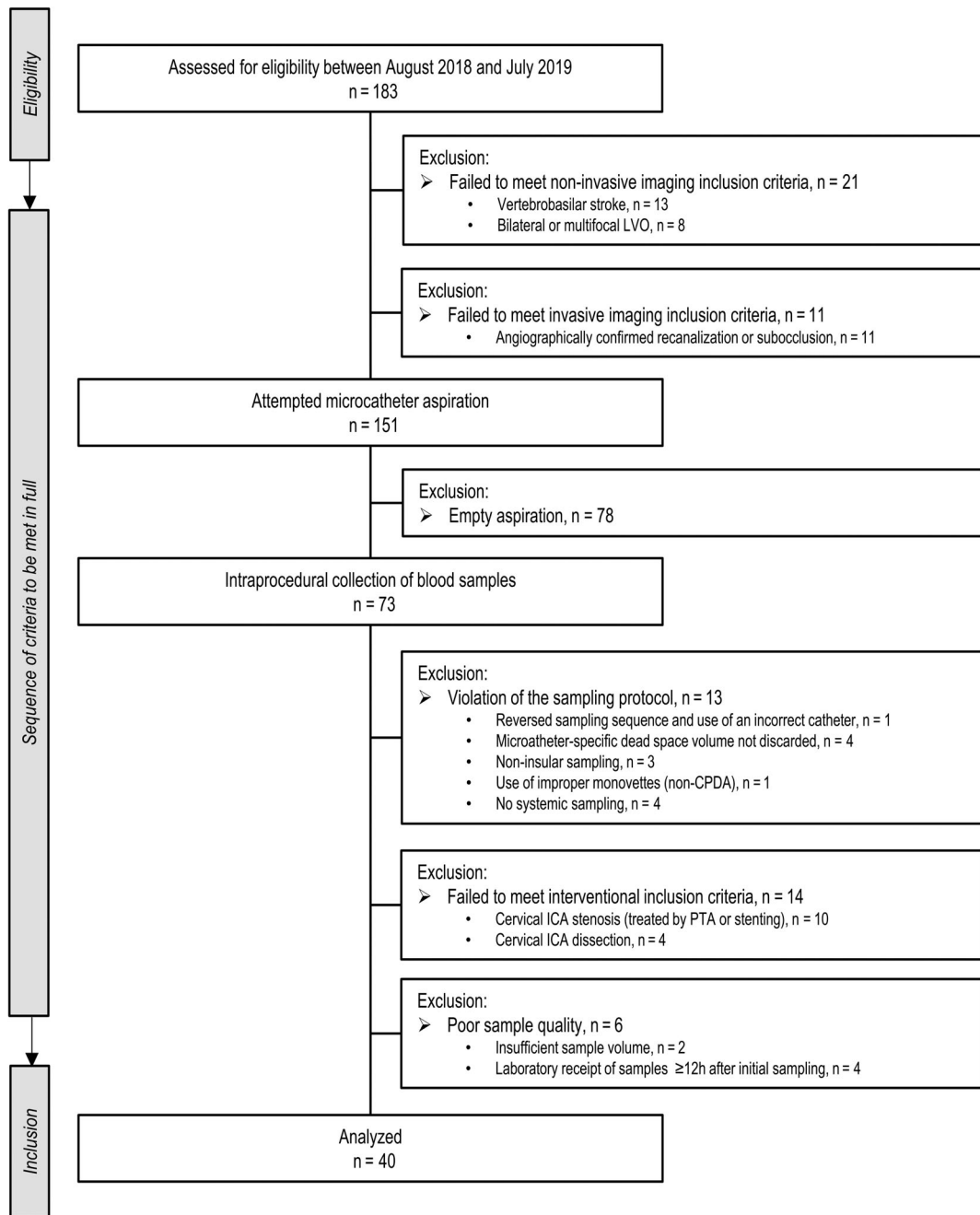
Eligibility

Assessed for eligibility between August 2018 and July 2019
n = 183

Exclusion:
➢ Failed to meet non-invasive imaging inclusion criteria, n = 21
  • Vertebrobasilar stroke, n = 13
  • Bilateral or multifocal LVO, n = 8

Exclusion:
➢ Failed to meet invasive imaging inclusion criteria, n = 11
  • Angiographically confirmed recanalization or subocclusion, n = 11

Attempted microcatheter aspiration
n = 151

Exclusion:
➢ Empty aspiration, n = 78

Intraprocedural collection of blood samples
n = 73

Exclusion:
➢ Violation of the sampling protocol, n = 13
  • Reversed sampling sequence and use of an incorrect catheter, n = 1
  • Microatheter-specific dead space volume not discarded, n = 4
  • Non-insular sampling, n = 3
  • Use of improper monovettes (non-CPDA), n = 1
  • No systemic sampling, n = 4

Exclusion:
➢ Failed to meet interventional inclusion criteria, n = 14
  • Cervical ICA stenosis (treated by PTA or stenting), n = 10
  • Cervical ICA dissection, n = 4

Exclusion:
➢ Poor sample quality, n = 6
  • Insufficient sample volume, n = 2
  • Laboratory receipt of samples ≥12h after initial sampling, n = 4

Sequence of criteria to be met in full

Inclusion

Analyzed
n = 40

FIGURE 1: Flowchart of patient inclusion. CPDA = citrate–phosphate–dextrose–adenine; ICA = internal carotid artery; LVO = large vessel occlusion; PTA = percutaneous transluminal angioplasty.

catheter-associated thrombus formation. None of the included patients received heparin intravenously. A detailed description of the standard mechanical thrombectomy procedure has been provided previously.[30] Briefly, our institutional standard recommends stent–embolus retrieval in conjunction with the distal aspiration technique. This step is preceded by microwire and microcatheter penetration of the embolus and navigation into the midinsular M2 segment located within the center of the ischemic circulation. Importantly, during this moment, the embolic occlusion persists.

In total, the following 3 arterial blood sample triplicates were drawn by microcatheter aspiration: (1) distal to the embolus under occlusive condition (labeled as D) as well as under physiological antegrade blood flow, (2) in the cervical ICA (labeled as C), and (3) the external iliac artery/CFA (labeled as F). Specifically, the first sample (D, target position in the pial midinsular M2 segment) was obtained in the following manner (Fig 2 and Supplementary Videos 1 and 2). Before deploying the stent-retrieval device, and immediately after embolus penetration, a
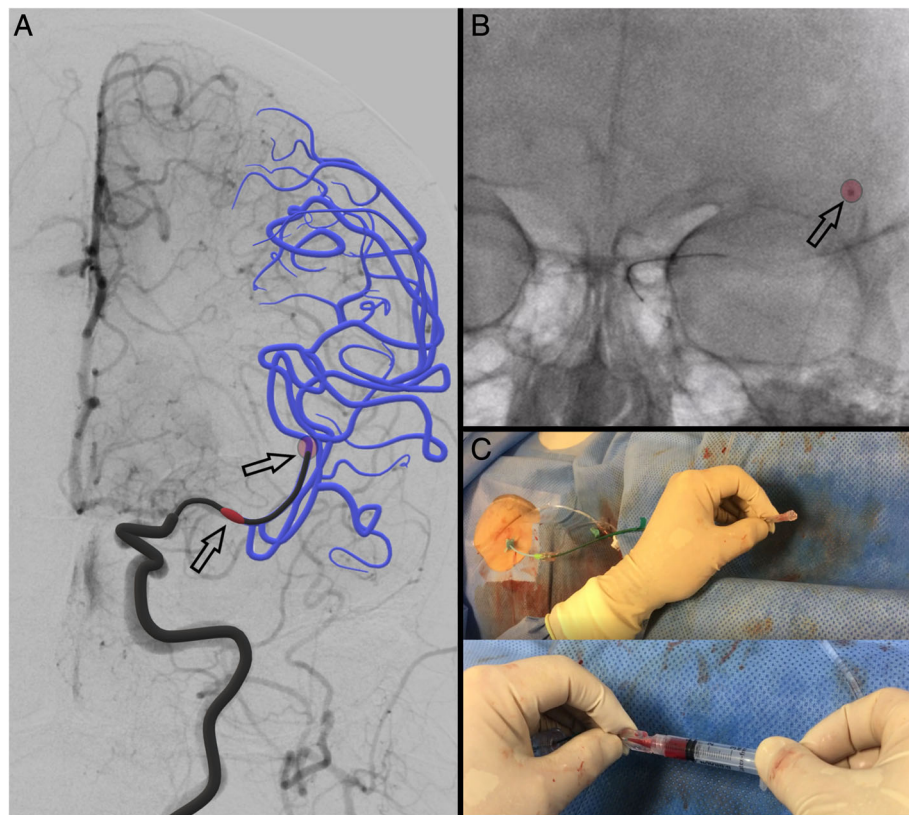
FIGURE 2: Sampling technique. (A) Digital subtraction angiography of the left ICA displaying embolic occlusion of the M1 segment of the MCA (red, *left black arrow*). Illustration: sampling situation in which postembolic/-occlusive blood flow in downstream vessels is substantially impaired (indigo), intermediate (proximal to embolic occlusion), and microcatheter (distal to embolic occlusion) in place (black). The desired sampling location in the M2 segment of the MCA is illustrated as a red circle *(right black arrow)*. **(B)** Left ICA angiogram of the same patient with appropriate microcatheter tip position in the M2 segment (red circle, *black arrow*). Animated fluoroscopic views of microcatheter navigation and its position during blood withdrawal are demonstrated by Supplementary Video 1. **(C)** Subtle back-bleeding after microwire removal (upper image) confirms the free intraluminal microcatheter position, followed by blood aspiration with a 3ml luer-lock syringe according to the sampling protocol. Blood withdrawal at the proximal end of the microcatheter is demonstrated by Supplementary Video 2. ICA = internal carotid artery; MCA = middle cerebral artery.

microcatheter of either 0.027in (Neuroslider 27; Acandis, Pforzheim, Germany) or 0.021in (Neuroslider 21, Acandis, and Rebar 18, Medtronic, Irvine, CA) inner lumen diameter was introduced beyond the occlusion site to obtain blood samples under occlusive ischemic condition. In general, it is medically necessary to leave it to the discretion of the operator whether a 0.027in or a 0.021in microcatheter needs to be used for the successful endovascular navigation to the target site. This therapeutic decision is typically guided by the tortuosity and the specific caliber of the paraophthalmic, the terminal ICA segment, and also the patient-specific anatomical variants of the first and/or second order MCA branches. After microcatheter positioning, the specific microcatheter dead space volume was aspirated with a 3ml luer-lock syringe and discarded (0.027in = 0.7ml dead space, 0.021in = 0.5ml dead space). Subsequently, a sample of 1ml of ischemic blood was drawn for laboratory analyses. The sample was then immediately transferred into a

5.6ml citrate–phosphate–dextrose–adenine (CPDA-1) monovette (S-Monovette; Sarstedt, Nümbrecht, Germany) and inverted manually 5 to 6 times to ensure that the anticoagulant was evenly dispersed.

After recanalization (mTICI), the samples of systemic arterial blood (C and F) were analogously drawn by aspiration using the exact same microcatheter as for D. For sample processing and laboratory analyses, a time window of a maximum of 12 hours after initial sampling (D) was allowed. When initial sampling was not possible, the patient was excluded from the study, and the standard mechanical thrombectomy procedure was continued without any significant delay. We did not intend peripheral venous sampling, which was not part of our study protocol and ethical vote.

Terminology

Throughout this article the terms "pial artery" or "pial artery segment" are applied to the first- and second-order

MCA branches, which are located at the pial brain surface. Pial blood sampling through microcatheter aspiration was performed in the insular M2 segment region immediately distal to the occlusive embolus and not from further distal branches or from within the microcirculation, the latter of which is technically not possible. Because the precise locations studied here corresponded to ICA-T/M1 and proximal M2 embolic occlusions, microcatheter sampling by aspiration was from a uniquely sealed macrovascular compartment into which blood flow during persisting occlusion condition is fed through pial collateral channels, which connect the terminal branches of the occluded vascular MCA field with the adjacent anterior cerebral artery (ACA) and posterior cerebral artery (PCA) territories.[31]

Laboratory Analysis

Leukocyte and Platelet Analyses. Sample processing and analyses were performed by trained laboratory technicians blinded to clinical data. CPDA-anticoagulated whole blood samples of the different arterial regions were used for cell counting and the preparation of blood smears. Cell counting was performed after red blood cell lysis and white blood cell (WBC) staining with Tuerk solution (Merck, Darmstadt, Germany) using a Fuchs-Rosenthal counting chamber. To prepare blood smears, a blood droplet (5μl) from whole blood samples was placed on glass slides (R. Langenbrinck, Emmendingen, Germany) and gently spread using the edge of a second glass slide. For histological staining, blood smears were air dried and stained by standard Pappenheim stain (Merck). The numbers of blood monocyte, lymphocyte, and neutrophil granulocyte counts were calculated by multiplying the percentages in Pappenheim-stained blood smears with the respective WBC counts. The number of platelet counts was determined by obtaining an average of the number of platelets in the Pappenheim-stained blood smears (5 fields of view) at ×100 magnification (oil immersion) multiplied by 20,000 to yield a platelet count estimate per microliter.[32]

Plasma Preparation. To remove cells from plasma, CPDA-treated blood samples were centrifuged for 10 minutes at $1,000 \times g$. The resulting supernatant (plasma) was immediately stored at −20°C.

Chemokine/Cytokine Quantification. We quantified the concentrations of IL-8, IP-10, Eotaxin, TARC, MCP-1, RANTES, MIP-1a, MIG, CXCL-5 (ENA-78), MIP-3a, GROa, CXCL-11 (I-TAC), and MIP-1b in plasma samples by a fluorescent bead immunoassay (LEGENDplex; Biolegend, San Diego, CA) according to the manufacturer's instructions.

Statistical Analysis

Statistical analyses were performed using GraphPad Prism 8.2.1 (GraphPad Software, San Diego, CA) and MedCalc 19.1 (MedCalc Software, Ostend, Belgium), including 1-way analysis of variance (ANOVA) followed by Tukey multiple comparison test, 2-way ANOVA followed by Sidak multiple comparison test, and Friedman rank test followed by Dunn multiple comparison test, as indicated in the text. Data are given as mean with 95% confidence interval (CI), as median with interquartile range (IQR), or absolute and relative frequency distribution, unless otherwise specified. Variables of univariate association ($p < 0.05$) were chosen for entry into multiple logistic regression. Stepwise selection procedures were used to fit a model to these variables. A 2-sided p value of <0.05 was considered to indicate statistical significance.

Results

Between August 2018 and July 2019, 183 consecutive patients with LVO stroke were assessed for study eligibility (see Fig 1). According to the applied prospective protocol, 32 patients failed to meet noninvasive and invasive imaging inclusion criteria due to vertebrobasilar stroke (n = 13), multifocal vessel occlusion (n = 8), and angiographically confirmed vessel recanalization or vessel subocclusion (n = 11). Therefore, 151 patients underwent mechanical thrombectomy for anterior circulation LVO at the following target sites: ICA-T, M1, and proximal M2. Microcatheter aspiration of ischemic blood was attempted in all 151 patients. The aspiration of 1ml of ischemic blood succeeded in 73 of 151 patients. Thirty-three of these 73 patients were excluded due to the following protocol violations: n = 1, reversed sampling sequence (initial systemic sampling) and use of an incorrect sampling catheter; n = 4, microcatheter-specific dead space volume was not discarded; n = 3, noninsular sampling (ie, not within an M2 vessel segment distal to the occlusion site); n = 1, use of improper monovettes (non-CPDA); n = 4, no systemic sampling; n = 10, cervical ICA stenosis >50% treated by PTA or stenting; n = 4, cervical vessel dissection (either at baseline or occurring during the procedure); n = 2, insufficient sample volume (<1ml after discarding the dead space volume); n = 4, laboratory receipt of samples beyond >12 hours after initial sampling. Thus, a total of 120 samples of 40 patients entered laboratory analyses (see Fig 1).

The demographic, clinical, imaging, interventional, and sampling-related patient characteristics of the study cohort are presented in Table 1. Briefly, median patient age was 76 years (IQR = 69–83 years), and sex was similarly distributed (40% men, 60% women). The most

TABLE 1. Demographic, Clinical, Imaging, Interventional, and Sampling-Related Patient Characteristics (N = 40)

Demographics	Value
Age, yr, median (IQR)	76 (69–83)
Male sex, n (%)	16 (40%)
Medical history, n (%)	
Hypertension	32 (40)
Diabetes mellitus	7 (18)
Hyperlipidemia	6 (15)
Atrial fibrillation	20 (50)
Current smoker	5 (13)
Baseline medication, n (%)	
Antithrombotic medication	20 (50)
Antihypertensive drugs	32 (80)
Clinical presentation	
Systolic blood pressure, mmHg, median (IQR)	160 (150–180)
Diastolic blood pressure, mmHg, median (IQR)	90 (77–95)
Heart rate, min^{-1}, median (IQR)	78 (67–87)
NIHSS at presentation, median (IQR)	14 (8–17)
Unknown time of symptom onset, n (%)	9 (23)
Baseline ASPECTS, median (IQR)	8 (7–9)
Collateral status, median (IQR)	2 (1–3)
Treatment	
IV rt-PA, n (%)	14 (35)
Intervention	
Onset-to-puncture, min, median (IQR)	253 (168–298)
Angiographic occlusion location[a]	
M1, n (%)	27 (68)
M2, n (%)	11 (28)
ICA, n (%)	9 (23)
Stent-retrieval maneuvers, median (IQR)	2 (1–3)
Successful recanalization, n (%)	35 (88)
Onset-to-recanalization time, min, median (IQR)	325 (250–378)
Sampling, median (IQR)	
Onset-to-distal sampling time, min	300 (200–350)
Onset-to-carotid sampling time, min	325 (240–378)
Onset-to-femoral sampling time, min	330 (257–384)
Last sampling-to-sample processing time	49 (29–170)
Outcome	
ASPECTS 48 hours postintervention, median (IQR)	7 (6–8)
NIHSS 72 hours postintervention, median (IQR)	5 (2–14)
Symptomatic intracranial hemorrhage, n (%)	6 (15)
In-house mortality, n (%)	5 (13)

Values are presented as number (percentage) for categorical variables and median (IQR) for continuous variables.

[a]Including combined vessel occlusions.

ASPECTS = Alberta Stroke Program Early CT Score; ICA = internal carotid artery; IQR = interquartile range; IV rt-PA = intravenous recombinant tissue plasminogen activator; NIHSS = National Institutes of Health Stroke Scale; M1/M2 = middle cerebral artery section.

prevalent comorbid disease was atrial fibrillation (50%), followed by hypertension (40%). Median NIHSS at presentation was 14 (IQR = 8–17). The median preprocedural ASPECTS at presentation was 8 (IQR = 7–9), along with a median collateral score of 2 (IQR = 1–3). Fourteen patients (35%) received IV rt-PA treatment before the endovascular procedure. The median time from symptom onset to groin puncture was 253 minutes (IQR = 168–298). On the initial angiogram, 27 (68%) patients showed M1 occlusion, 9 (23%) an ICA-T, and 11 (28%) a proximal M2 occlusion, respectively (including combined vessel occlusions). The median time from symptom onset to initial blood sampling (D) was 300 minutes (IQR = 200–350), and the median time from last sampling to sample processing was 49 minutes (IQR = 29–170). Technically successful recanalization (defined as mTICI 2b or 3) was achieved in 35 patients (88%) after a median of 2 (IQR = 1–3) stent-retrieval maneuvers and a median time after symptom onset of 325 minutes (IQR = 250–378). No peri-interventional complications (eg, thrombus fragmentation or vessel perforation) were observed. Median postprocedural ASPECTS (48 hours after recanalization therapy) was 7 (IQR = 6–8). At 72 hours postintervention, 26 (65%) patients showed clinical improvement after recanalization therapy equivalent to an NIHSS drop (median) to 5 (IQR = 2–14). Symptomatic intracranial hemorrhage was observed in 6 (15%) patients. Five (13%) patients died during the hospital stay.

Total and differential leukocyte as well as platelet counts were determined in the obtained blood samples and are given in Figure 3. The total number of leukocytes was significantly increased under occlusion condition (D) as compared with the carotid (C) and femoral (F) control samples obtained under uncompromised arterial flow (D: 5,927/µl, 95% CI = 5,066 to 6,788 vs C: 5,148/µl, 95% CI = 4,444 to 5,852, p = 0.0003; D vs F: 4,873/µl, 95% CI = 4,136 to 5,611, p < 0.0001). This difference in the total leukocyte counts was primarily attributable to a significant and strong increase in the neutrophil subpopulation (D: 5,152/µl, 95% CI = 4,261 to 6,042 vs C: 4,556/µl, 95% CI = 3,859 to 5,253, p = 0.0018; D vs F: 4,342/µl, 95% CI = 3,619 to 5,064, p = 0.00039). Data also showed a significant increase for both the lymphocyte and monocyte subpopulation (postocclusive lymphocyte accumulation with D: 509/µl, 95% CI = 391 to 627 vs C: 470/µl, 95% CI = 362 to 579, p = 0.3922; D vs F: 409/µl, 95% CI = 335 to 483 p = 0.0225; postocclusive monocyte accumulation with D: 200/µl, 95% CI = 144 to 255 vs C: 168/µl, 95% CI = 123 to 213, p = 0.3109 and D vs F: 153/µl, 95% CI = 121 to 184, p = 0.0316). No differences in platelet counts were found between the 3 sampling locations (D: 346,843/µl, 95% CI = 273,663 to 419,992 vs C: 351,896/µl, 95% CI = 283,522 to 420,270, p > 0.9999; D vs F: 330,106/µl, 95% CI = 268,656 to 391,556, p > 0.9999). There were no significant differences in leukocytes or platelets between the 2 control locations under physiological flow condition (sampling locations C vs F).

Ischemic-to-systemic leukocyte cell count ratios were calculated by dividing the distal cell count per subpopulation by the mean systemic cell count per subpopulation (given as percentage) to adjust for interindividual variations and used to determine the association between relative changes in ischemic immune cell counts and clinical outcome (NIHSS at 72 hours).[33] Univariate regression analysis (Fig 4) revealed that outcome was only associated with relative changes in neutrophil counts (β coefficient = 0.101, 95% CI = 0.0063 to 0.1957, p = 0.0373). However, no association was found for lymphocytes (β coefficient = 0.0403, 95% CI = −0.0409 to 0.1215, p = 0.3199) or monocytes (β coefficient = −0.0062, 95% CI = −0.05 to 0.0377, p = 0.7769).

Plasmatic chemokine levels were determined to assess leukocyte attraction to the ischemic circulation and are given in Figure 5 and Table 2. Significantly elevated levels were detected only for CXCL-11 (see Fig 5) in the postocclusive samples as compared with the femoral sampling location (D: 144.5pg/ml, 95% CI = 104.7 to 184.2 vs C: 131.3pg/ml, 95% CI = 96.48 to 166.2, p = 0.1536; D vs F: 120.3pg/ml, 95% CI = 84.08 to 156.5, p = 0.0027). By contrast, no significant variations were seen for all other chemokines/cytokines (see Table 2) or between the 2 control samples (C and F).

Secondary Analyses

Multiple logistic regression analysis was performed to identify principal patient characteristics influencing the ability to obtain ischemic blood aspirates (binary outcome of successful vs unsuccessful aspiration). A model covering all patient characteristics assessed by the time of attempted sampling (ie, age, sex, hypertension, diabetes mellitus, hyperlipidemia, smoking, antithrombotic medication, antihypertensive medication, blood pressure, heart rate, NIHSS at presentation, unknown time of symptom onset, ASPECTS at presentation, CT angiography collateral status, IV thrombolysis, and the time interval from symptom onset to groin puncture) revealed that only active smoking (adjusted odds ratio [OR] = 0.3863, 95% CI = 0.1568 to 0.9515, p = 0.0386) and collateral status (adjusted OR = 1.7131, 95% CI = 1.0694 to 1.9395, p = 0.0252) were predictive of whether sampling failed or succeeded.

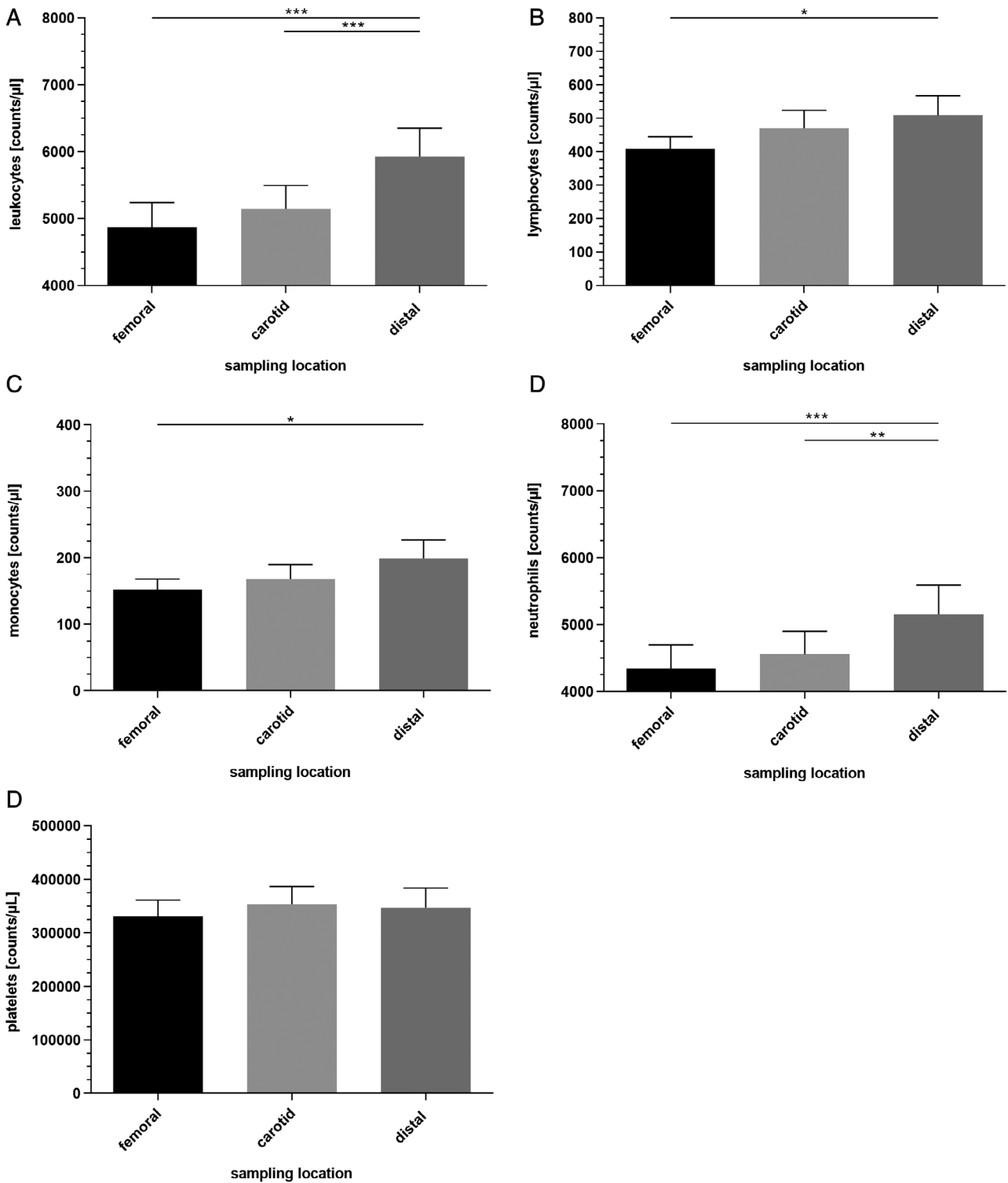Cell count profiles with regard to IV thrombolysis (rt-PA) are given in Table 3. Our main finding of an

FIGURE 3: Total leukocyte counts (A), differential leukocyte counts (B, C) and platelet counts (E) of local occlusive versus systemic arterial blood in ischemic stroke, labeling according to the sampling location. Data are given as mean ± standard error of the mean. Friedman test with Dunn post hoc test; *p < 0.05, **p < 0.005, ***p < 0.0005; n = 40 (A)/n = 37 (B–E; triplicates F/C/D).

ischemic leukocyte accumulation was independent from rt-PA status. However, the overall level of leukocyte cell counts was higher in the rt-PA versus the non–rt-PA group and mainly driven by neutrophils (rt-PA D: 6391/μl, 95% CI = 4,615 to

8,147 vs non–rt-PA D: 4,452/μl, 95% CI = 3,560 to 5,343, p = 0.028; rt-PA C: 5,529/μl, 95% CI = 4,205 to 6,853 vs non–rt-PA C: 3,972/μl, 95% CI = 3,248 to 4,697, p = 0.0.0863; rt-PA F: 5,436/μl, 95% CI = 4,093 to 6,779
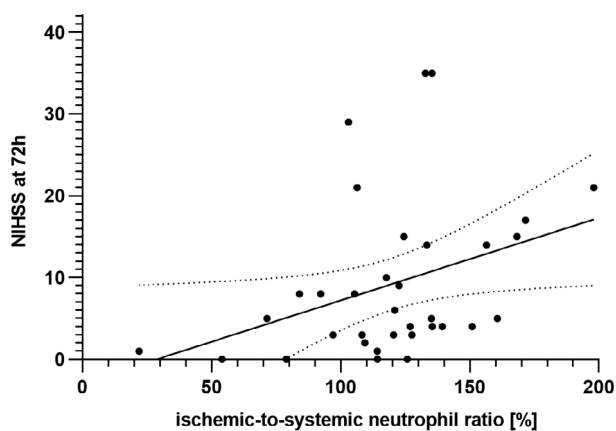
FIGURE 4: Association of distal (occlusive) neutrophil recruitment and National Institutes of Health Stroke Scale (NIHSS) at 72 hours postintervention. The 95% confidence interval (CI) is given as short dotted lines. $\beta = 0.101$, 95% CI = 0.0063–0.1957, $R^2 = 0.13$, $p = 0.0373$.
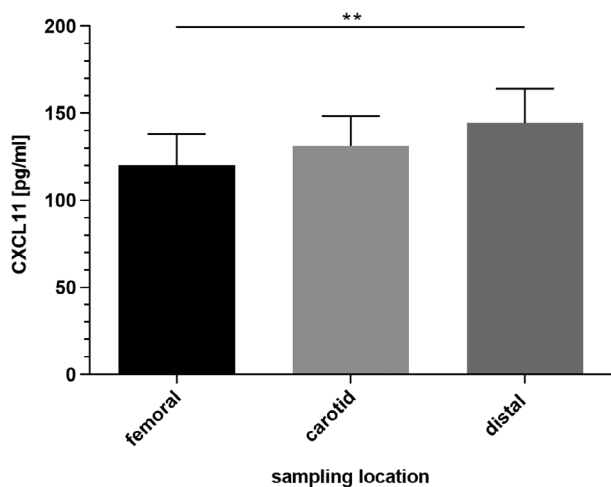

FIGURE 5: Plasma levels of CXCL-11 local occlusive versus systemic arterial blood in ischemic stroke, labeling according to the sampling location. Samples correspond with the samples in Figure 3. Data are given as mean ± standard error of the mean. One-way analysis of variance with Tukey multiple comparison test; **$p < 0.005$; $n = 37$ (triplicates F/C/D).

vs non–rt-PA F: 3,749/μl, 95% CI = 2,934 to 4,564, $p = 0.0794$).

Discussion

In this study, we show that microcatheter aspiration in the course of mechanical thrombectomy allows for direct probing of the ischemic arterial compartment during the hyperacute stage of cerebral arterial occlusion in humans. We have used this innovative technique to investigate local cellular and molecular alterations during (hyper)acute ischemic stroke in postocclusive blood (ie, distal to the occlusion site) to gain insights into early ischemia-induced pathophysiological

events in the human brain. Employing this method, our most relevant findings can be summarized as follows: (1) a significant increase in the total number of leukocytes, (2) which was primarily attributable to a significant and strong elevation of the neutrophil subpopulation within the occluded vascular compartment; a significant increase in (3) lymphocyte and (4) monocyte counts; (5) a corresponding increase in the expression of the activated T-cell chemoattractant CXCL-11, and finally (6) a significant association of relative changes in ischemic neutrophil counts with outcome. These observations were made strictly during complete vascular occlusion, immediately distal to the occlusion site and before recanalization. For the precise occlusion locations that were studied here, the collateral blood flow entering the occluded ischemic field is fed by pial collateral channels connecting the occluded MCA with the adjacent ACA and PCA territories.[31] Therefore, it can be reasoned that the likely entry route of the observed leukocellular invasion was via retrograde collateral pial blood flow. Other conceivable explanations are (1) a selective local passive enrichment through physical trapping or (2) migration from microvascular sites. However, we consider passive enrichment less likely because the observed increase in cell counts was not isolated to a single leukocyte subpopulation and, by contrast, could not be observed for platelets. Likewise, we also consider cellular migration a less plausible explanation because neutrophils are not found to reside predominantly in the brain,[34] and their migration would have to be directed against significant forces of the blood stream and over a considerable distance at the same time (into the macrovascular M2 site of sampling).

To accomplish these observations, it was essential to establish a rigorous protocol for intraprocedural ischemic blood sampling followed by timely laboratory analyses in the direct vicinity of the interventional angiography room. Strict selection criteria were applied to ensure homogeneity of the study population and the comparability with common experimental stroke models.[24]

Based on the data presented here, it is now possible to draw close parallels to seminal experimental observations made 3 decades ago. Hallenbeck and colleagues reported remarkably similar findings in a canine model.[19] The authors used a double-label autoradiography technique to correlate both the local cerebral blood flow (^{14}C-iodoantipyrine) and accumulations of ^{111}indium-oxine–labeled granulocytes at different time points after focal ischemia, observing early punctuate granulocyte clustering in brain regions with low blood flow. This work led Hallenbeck and others to the conclusion that thrombotic and inflammatory pathways might converge during early phases of cerebral ischemia.[19,20,35] Our data provide the first direct human observation strongly supportive of the

TABLE 2. Plasmatic Cytokine and Chemokine Concentrations

	Mean, pg/ml (95% CI)			Mean Difference, pg/ml (95% CI)			
	F	C	D	F/C	F/D	C/D	p
IL-8	215.5 (106.6 to 324.6)	233.2 (96.38 to 370.1)	207.1 (100.3 to 313.8)	−17.8 (−60.88 to 25.27)	8.352 (−38.33 to 55.03)	26.16 (−33.24 to 85.56)	0.42
IL-10	11.65 (6.11 to 17.19)	10.99 (5.92 to 17.05)	22.61 (−9.99 to 55.21)	0.66 (−4.06 to 5.38)	−10.96 (−46.63 to 24.72)	−11.62 (−51.56 to 28.31)	0.47
Eotaxin	165.6 (140.8 to 190.5)	169.7 (144.4 to 194.9)	174.3 (146.8 to 201;8)	−4.5 (−13.84 to 5.74)	−8.73 (−22.6 to 5.15)	−4.68 (−15.51 to 5.16)	0.19
TARC	123.9 (88.54 to 159.3)	133.4 (102.1 to 164.8)	128.7 (96.74 to 160.6)	−9.49 (−21.17 to 2.17)	−4.72 (−17.76 to 8.31)	4.78 (−6.33 to 15.88)	0.16
MCP-1	548.5 (425.2 to 671.7)	533.1 (430.2 to 636.0)	559.4 (424.6 to 694.2)	15.39 (−26.3 to 57.08)	−10.93 (−68.32 to 46.45)	−26.32 (−101.5 to 48.81)	0.5
RANTES	1081 (693.1 to 1468)	1013 (682.7 to 1342)	1062 (721.5 to 1403)	68.15 (−138.1 to 274.4)	18.19 (−214.8 to 251.2)	−49.97 (−182.9 to 82.96)	0.62
MIP-1a	548.5 (425.1 to 671.7)	533.1 (430.2 to 636.0)	559.4 (424.6 to 694.2)	15.39 (−26.30 to 57.08)	−10.93 (−68.32 to 46.45)	−26.32 (−101.5 to 48.81)	0.5
MIG	154.9 (82.92 to 226.8)	141 (69.57 to 212.4)	140.8 (69.27 to 212.3)	13.87 (−19.18 to 46.93)	14.09 (−33.98 to 62.15)	0.21 (−48.97 to 49.4)	0.64
CXCL-5	44.78 (33.49 to 56.07)	47.33 (32.04 to 62.63)	45.24 (30.89 to 59.6)	−2.56 (−12.25 to 7.14)	−0.46 (−7.09 to 6.17)	2.09 (−7.02 to 11.2)	0.71
MIP-3a	42.62 (19.16 to 66.08)	31.94 (17.57 to 46.31)	32.82 (19.22 to 46.4)	10.68 (−11.86 to 33.22)	9.8 (−13.26 to 32.87)	−0.88 (−6.12 to 4.36)	0.28
GROa	142.9 (69.87 to 215.9)	129 (61.9 to 196)	137.7 (64.58;210.8)	13.92 (−103.6 to 131.4)	5.19 (−112.3 to 122.7)	−8.72 (−125.2 to 107.8)	0.96
MIP-1b	50.92 (22.87 to 78.97)	47.86 (23.52 to 72.2)	47.59 (19.34 to 75.84)	3.07 (−2.66 to 8.79)	3.33 (−3.05 to 9.72)	0.27 (−7.38 to 7.91)	0.37

One-way analysis of variance with Tukey multiple comparison test, n = 37 (conditions F/C/D).
Arterial plasma levels of IL-8, IL-10, Eotaxin (CCL11), TARC, MCP-1, RANTES, MIP-1a, MIG, CXCL-5 (ENA-78), MIP-3a, GROa, and MIP-1b in ischemic stroke, labeling according to the sampling location. Samples correspond with the samples in Figures 3 and 5.
CI = confidence interval.

pathophysiological concept that a very early innate immune response is operative in ischemic stroke. In experimental stroke, early accumulation of neutrophils in the ischemic vasculature has been described in great detail.[36] Briefly, a key step in the very early ischemic cascade is represented by endothelial adhesion of both leukocytes and platelets.[37]

Among leukocytes, neutrophils are 1 of the first immune cells to rise within the peripheral circulation hours after ischemic stroke onset, being associated with stroke severity as well as worse functional outcome.[38,39] As shown by an earlier study using technetium-99m hexamethylpropyleneamine oxime−labeled leukocytes,

neutrophils were dynamically recruited to the ischemic human brain; however, the precise timing and route of neutrophil accumulation remained unclear.[40] Once in situ, they appear to be involved in a local cytokine and cell adhesion molecule–driven inflammatory response constituted by the activation of the luminal endothelial surface, neutrophil rolling, adhesion, as well as blood–brain barrier (BBB) disruption and finally neutrophil migration and crossing into the infarcted tissue.[20,36,41] In models of transient cerebral ischemia with reperfusion, leukocytes, and particularly neutrophils, accumulate in small arterioles and postcapillary venules, and in concert with platelets partly obstruct the microvascular bed.[19,20]

TABLE 3. Differences in Immune Cell and Platelet Counts Between rt-PA and Non–rt-PA Patients

	rt-PA, Counts/μl, Mean (95% CI)	Non–rt-PA, Counts/μl, Mean (95% CI)	Mean Difference (95% CI)	p
Leukocytes				
Femoral	5,693 (4,180 to 7,207)	4,432 (3,610 to 5,252)	1,262 (−601 to 3,125)	0.2795
Carotid	6,176 (4,755 to 7,598)	4,594 (3,839 to 5,349)	1,583 (−281 to 3,446)	0.1203
Distal	7,076 (5,225 to 8,928)	5,309 (4,422 to 6,195)	1,768 (−95 to 3,631)	0.0683
Lymphocytes				
Femoral	435 (325 to 546)	395 (293 to 496)	41 (−217 to 298)	0.9733
Carotid	437 (321 to 554)	490 (331 to 650)	−56 (−314 to 201)	0.9344
Distal	452 (355 to 549)	544 (367 to 722)	−101 (−359 to 156)	0.7148
Monocytes				
Femoral	187 (119 to 256)	134 (100 to 168)	53 (−55 to 161)	0.5519
Carotid	222 (117 to 328)	137 (103 to 171)	87 (−21 to 195)	0.149
Distal	275 (159 to 391)	158 (106 to 210)	119 (10 to 227)	0.0267
Neutrophils				
Femoral	5,436 (4,093 to 6,779)	3,749 (2,934 to 4,564)	1,687 (−145 to 3,520)	0.0794
Carotid	5,529 (4,205 to 6,853)	3,972 (3,248 to 4,697)	1,661 (−172 to 3,494)	0.0863
Distal	6,391 (4,615 to 8,147)	4,452 (3,560 to 5,343)	1,992 (160 to 3,825)	0.028
Platelets				
Femoral	336,615 (217,306 to 455,925)	340,333 (265,963 to 414,703)	−3,718 (−174,492 to 167,056)	>0.9999
Carotid	362,154 (194,799 to 529,509)	361,000 (295,494 to 426,506)	1,154 (−169,620 to 171,928)	>0.9999
Distal	347,077 (187,689 to 506,464)	361,167 (278,925 to 443,408)	−14,090 (−184,864 to 156,684)	0.996

Two-way analysis of variance with Sidak multiple comparison test; rt-PA, n = 14 (conditions F/C/D); non–rt-PA, n = 26 (triplicates F/C/D). Differences in arterial cell counts between rt-PA and non–rt-PA patients in ischemic stroke, labeling according to the sampling location. Samples correspond with the samples in Figures 3 and 5.

CI = confidence interval; rt-PA = recombinant tissue plasminogen activator.

Currently, there are no human data on local, very early inflammatory processes immediately after and during vascular occlusion in the ischemic arterial compartment.[37,42] Studies in human ex vivo specimens to date have provided a rough spatiotemporal characterization of the dynamics of cerebral leukocyte infiltration at intervals from day 1 after the ictus to 53 years, sparing the (hyper) acute phase.[16,17,43] By direct local and in vivo human observation, we now provide evidence that supports the notion of a predominantly intravascular accumulation of neutrophils in the very early occlusive stage of human stroke and present the first data attesting to the association

of acute postocclusive changes in neutrophil counts and outcome. However, we were unable to identify a potential molecular driver of neutrophil attraction using the selected inflammatory chemokine panel.

Interestingly, subgroup analysis indicates that IV rt-PA administration induced an overall increase of leukocytes in rt-PA versus non–rt-PA patients. It is known that rt-PA administration in acute ischemic stroke leads to the upregulation of matrix metalloproteinase 9 (MMP-9), which in turn is a major contributor to BBB degradation and hemorrhagic complications.[44,45] Although there is a complex and ongoing debate about the exact type of

(immune)cell responsible for this increase, neutrophils can be identified as candidates of being the relevant source of MMP-9 increase following rt-PA administration.[46] In line with the literature, we found that immune cell patterns and particularly neutrophils seem to be modulated by rt-PA administration. However, the precise functional role of neutrophils at different stages of stroke development and their net effect on stroke outcome is a matter of ongoing research and controversies remain (reviewed in detail elsewhere).[47]

The neutrophilic invasion appears to be accompanied by a significant but less pronounced influx of lymphocytes and monocytes, which is supportive of the concept that the immune response to ischemic stroke commences already during the early stage of vascular occlusion and might evolve sequentially.[37] In experimental stroke, there is compelling evidence that T lymphocytes contribute to infarct development in an antigen-independent manner.[47] Consistently, immunodeficient $Rag1^{-/-}$ mice lacking T and B cells were shown to be protected from ischemia/reperfusion injury (I/R) after transient middle cerebral artery occlusion (tMCAO), and reconstitution of $Rag1^{-/-}$ animals with donor T cells by adoptive transfer reversed protection.[12,13] These encouraging findings have already led to experimental and pilot clinical stroke trials with FTY720,[48–50] an immunosuppressant licensed for the treatment of multiple sclerosis patients.[51] FTY720-induced lymphopenia ameliorates I/R injury after tMCAO in mice,[48] and also in patients when combined with alteplase and/or mechanical thrombectomy.[49,50] In addition, these stroke mitigating effects were also seen in a small cohort of acute stroke patients who could not be treated by IV thrombolysis or mechanical thrombectomy.[52] Our data for the first time show that the number of lymphocytes increases in the occluded vascular field in acute stroke patients and thereby strongly support the rationale for early adjunct anti-lymphocyte treatment. The significant increase of plasmatic CXCL-11 (I-TAC) levels in the cerebral circulation during (hyper)acute stroke further directs attention to lymphocellular influx in that CXCL-11 is a non-ELR chemokine, which has potent chemoattractant activity for activated T cells but not for unstimulated T cells, neutrophils, or monocytes.[53] The CXC chemokine subfamily is devided into ELR and non-ELR chemokines. The term ELR refers to the presence or absence of the Glu-Leu-Arg tripeptide sequence.

An observed limitation of the developed method was that sampling succeeded in only 73 out of 151 patients, in all of whom microcatheter aspiration was attempted. Of note, in a stepwise multiple logistic regression model with aspiration as a binary outcome (successful vs unsuccessful),

comprehensive clinical and imaging data clearly suggested that biological reasons, rather than, or at least in addition to technical reasons, might explain why aspiration fails in certain cases. Specifically, poor collateral and smoking status predicted whether aspiration succeeded.

In conclusion, this study provides the first direct evidence of an immediate immune response to ischemic stroke during the hyperacute stage of cerebral arterial occlusion in humans. We particularly demonstrate by local probing of pial ischemic blood that neutrophils, as part of the innate immune system, numerically dominate the cellular response and seem to affect outcome. In addition, we observed a significant influx of lymphocytes, which is potentially amenable to adjunct immunomodulatory therapy. Besides the quantification of the local inflammatory reaction by cell numbers and protein concentrations, the novel approach of probing the ischemic arterial compartment in the course of mechanical thrombectomy paves the way for investigations on cellular interaction and activation, such as of lymphocytes and platelets as driving forces of cerebral injury in experimental stroke.[54] Taken together, these findings may provide a key to bridging the gap between experimental stroke models and actual stroke patients.

Author Contributions

A.M.K., B.N., G.S., and M.P. contributed to the conception and design of the study. A.M.K., M.K.S., and M.P. contributed to the acquisition and analysis of data. All authors contributed to drafting the text and preparing the figures.

Potential Conflicts of Interest

Nothing to report.

References

1. GBD 2015 Neurological Disorders Collaborator Group. Global, regional, and national burden of neurological disorders during 1990-2015: a systematic analysis for the Global Burden of Disease Study 2015. Lancet Neurol 2017;16:877–897.

2. Powers WJ, Rabinstein AA, Ackerson T, et al. 2018 guidelines for the early management of patients with acute ischemic stroke: a guideline

for healthcare professionals from the American Heart Association/American Stroke Association. Stroke 2018;49:e46–e110.

3. Goyal M, Menon BK, van Zwam WH, et al. Endovascular thrombectomy after large-vessel ischaemic stroke: a meta-analysis of individual patient data from five randomised trials. Lancet 2016;387: 1723–1731.

4. Froehler MT, Saver JL, Zaidat OO, et al. Interhospital transfer before thrombectomy is associated with delayed treatment and worse outcome in the STRATIS Registry (Systematic Evaluation of Patients Treated With Neurothrombectomy Devices for Acute Ischemic Stroke). Circulation 2017;136:2311–2321.

5. de los Ríos la Rosa F, Khoury J, Kissela BM, et al. Eligibility for intravenous recombinant tissue-type plasminogen activator within a population. Stroke 2012;43:1591–1595.

6. Kollikowski AM, Amaya F, Stoll G, et al. Impact of landmark endovascular stroke trials on logistical performance measures: a before-and-after evaluation of real-world data from a regional stroke system of care. J Neurointerv Surg 2019;11:563–568.

7. Hussein HM, Saleem MA, Qureshi AI. Rates and predictors of futile recanalization in patients undergoing endovascular treatment in a multicenter clinical trial. Neuroradiology 2018;60:557–563.

8. van de Graaf RA, Chalos V, Del Zoppo GJ, et al. Periprocedural antithrombotic treatment during acute mechanical thrombectomy for ischemic stroke: a systematic review. Front Neurol 2018;9:238.

9. Khatri P, Wechsler LR, Broderick JP. Intracranial hemorrhage associated with revascularization therapies. Stroke 2007;38:431–440.

10. Brouns R, De Deyn PP. The complexity of neurobiological processes in acute ischemic stroke. Clin Neurol Neurosurg 2009;111:483–495.

11. Stoll G, Jander S, Schroeter M. Inflammation and glial responses in ischemic brain lesions. Prog Neurobiol 1998;56:149–171.

12. Yilmaz G, Arumugam T V, Stokes KY, Granger DN. Role of T lymphocytes and interferon-gamma in ischemic stroke. Circulation 2006; 113:2105–2112.

13. Kleinschnitz C, Schwab N, Kraft P, et al. Early detrimental T-cell effects in experimental cerebral ischemia are neither related to adaptive immunity nor thrombus formation. Blood 2010;115:3835–3842.

14. Chamorro Á, Meisel A, Planas AM, et al. The immunology of acute stroke. Nat Rev Neurol 2012;8:401–410.

15. Desilles J-P, Syvannarath V, Di Meglio L, et al. Downstream microvascular thrombosis in cortical venules is an early response to proximal cerebral arterial occlusion. J Am Heart Assoc 2018;7.

16. Mena H, Cadavid D, Rushing EJ. Human cerebral infarct: a proposed histopathologic classification based on 137 cases. Acta Neuropathol 2004;108:524–530.

17. Zrzavy T, Machado-Santos J, Christine S, et al. Dominant role of microglial and macrophage innate immune responses in human ischemic infarcts. Brain Pathol 2018;28:791–805.

18. Ames A, Wright RL, Kowada M, et al. Cerebral ischemia. II. The no-reflow phenomenon. Am J Pathol 1968;52:437–453.

19. Hallenbeck JM, Dutka AJ, Tanishima T, et al. Polymorphonuclear leukocyte accumulation in brain regions with low blood flow during the early postischemic period. Stroke 1986;17:246–253.

20. del Zoppo GJ, Mabuchi T. Cerebral microvessel responses to focal ischemia. J Cereb Blood Flow Metab 2003;23:879–894.

21. Stoll G, Kleinschnitz C, Nieswandt B. Combating innate inflammation: a new paradigm for acute treatment of stroke? Ann N Y Acad Sci 2010;1207:149–154.

22. Nieswandt B, Kleinschnitz C, Stoll G. Ischaemic stroke: a thrombo-inflammatory disease? J Physiol 2011;589:4115–4123.

23. Shichita T, Sugiyama Y, Ooboshi H, et al. Pivotal role of cerebral interleukin-17-producing gammadeltaT cells in the delayed phase of ischemic brain injury. Nat Med 2009;15:946–950.

24. Sommer CJ. Ischemic stroke: experimental models and reality. Acta Neuropathol 2017;133:245–261.

25. Smith EE, Kent DM, Bulsara KR, et al. Accuracy of prediction instruments for diagnosing large vessel occlusion in individuals with suspected stroke: a systematic review for the 2018 Guidelines for the Early Management of Patients With Acute Ischemic Stroke. Stroke 2018;49:e111–e122.

26. Chen W-T, Chang F-C, Huang H-C, et al. Total and differential leukocyte counts in ischemic stroke caused by vertebrobasilar artery dissection. J Neurol Sci 2019;404:101–105.

27. Welt FGP, Rogers C. Inflammation and restenosis in the stent era. Arterioscler Thromb Vasc Biol 2002;22:1769–1776.

28. Miteff F, Levi CR, Bateman GA, et al. The independent predictive utility of computed tomography angiographic collateral status in acute ischaemic stroke. Brain 2009;132(pt 8):2231–2238.

29. Zaidat OO, Yoo AJ, Khatri P, et al. Recommendations on angiographic revascularization grading standards for acute ischemic stroke: a consensus statement. Stroke 2013;44:2650–2663.

30. Humphries W, Hoit D, Doss VT, et al. Distal aspiration with retrievable stent assisted thrombectomy for the treatment of acute ischemic stroke. J Neurointerv Surg 2015;7:90–94.

31. Brozici M, van der Zwan A, Hillen B. Anatomy and functionality of leptomeningeal anastomoses: a review. Stroke 2003;34:2750–2762.

32. Malok M, Titchener EH, Bridgers C, et al. Comparison of two platelet count estimation methodologies for peripheral blood smears. Clin Lab Sci 2007;20:154–160.

33. Statland BE, Winkel P, Harris SC, et al. Evaluation of biologic sources of variation of leukocyte counts and other hematologic quantities using very precise automated analyzers. Am J Clin Pathol 1978;69: 48–54.

34. Kolaczkowska E, Kubes P. Neutrophil recruitment and function in health and inflammation. Nat Rev Immunol 2013;13:159–175.

35. Hallenbeck JM, Dutka AJ. Background review and current concepts of reperfusion injury. Arch Neurol 1990;47:1245–1254.

36. Jickling GC, Liu D, Ander BP, et al. Targeting neutrophils in ischemic stroke: translational insights from experimental studies. J Cereb Blood Flow Metab 2015;35:888–901.

37. Iadecola C, Anrather J. The immunology of stroke: from mechanisms to translation. Nat Med 2011;17:796–808.

38. Kim J, Song T-J, Park JH, et al. Different prognostic value of white blood cell subtypes in patients with acute cerebral infarction. Atherosclerosis 2012;222:464–467.

39. Kumar AD, Boehme AK, Siegler JE, et al. Leukocytosis in patients with neurologic deterioration after acute ischemic stroke is associated with poor outcomes. J Stroke Cerebrovasc Dis 2013;22: e111–e117.

40. Akopov SE, Simonian NA, Grigorian GS. Dynamics of polymorphonuclear leukocyte accumulation in acute cerebral infarction and their correlation with brain tissue damage. Stroke 1996;27:1739–1743.

41. Kataoka H, Kim S-W, Plesnila N. Leukocyte-endothelium interactions during permanent focal cerebral ischemia in mice. J Cereb Blood Flow Metab 2004;24:668–676.

42. Fraser JF, Collier LA, Gorman AA, et al. The Blood And Clot Thrombectomy Registry And Collaboration (BACTRAC) protocol: novel method for evaluating human stroke. J Neurointerv Surg 2019; 11:265–270.

43. Perez-de-Puig I, Miró-Mur F, Ferrer-Ferrer M, et al. Neutrophil recruitment to the brain in mouse and human ischemic stroke. Acta Neuropathol 2015;129:239–257.

44. Ning M, Furie KL, Koroshetz WJ, et al. Association between tPA therapy and raised early matrix metalloproteinase-9 in acute stroke. Neurology 2006;66:1550–1555.

45. Rosell A, Cuadrado E, Ortega-Aznar A, et al. MMP-9-positive neutrophil infiltration is associated to blood-brain barrier breakdown and basal lamina type IV collagen degradation during hemorrhagic transformation after human ischemic stroke. Stroke 2008;39:1121–1126.

46. Turner RJ, Sharp FR. Implications of MMP9 for blood brain barrier disruption and hemorrhagic transformation following ischemic stroke. Front Cell Neurosci 2016;10:56.

47. Strecker J-K, Schmidt A, Schäbitz W-R, Minnerup J. Neutrophil granulocytes in cerebral ischemia—evolution from killers to key players. Neurochem Int 2017;107:117–126.

48. Kraft P, Göb E, Schuhmann MK, et al. FTY720 ameliorates acute ischemic stroke in mice by reducing thrombo-inflammation but not by direct neuroprotection. Stroke 2013;44:3202–3210.

49. Zhu Z, Fu Y, Tian D, et al. Combination of the immune modulator fingolimod with alteplase in acute ischemic stroke. Circulation 2015;132:1104–1112.

50. Tian D-C, Shi K, Zhu Z, et al. Fingolimod enhances the efficacy of delayed alteplase administration in acute ischemic stroke by promoting anterograde reperfusion and retrograde collateral flow. Ann Neurol 2018;84:717–728.

51. Kappos L, Antel J, Comi G, et al. Oral fingolimod (FTY720) for relapsing multiple sclerosis. N Engl J Med 2006;355:1124–1140.

52. Fu Y, Zhang N, Ren L, et al. Impact of an immune modulator fingolimod on acute ischemic stroke. Proc Natl Acad Sci 2014;111:18315–18320.

53. Cole KE, Strick CA, Paradis TJ, et al. Interferon–inducible T cell alpha chemoattractant (I-TAC): a novel non-ELR CXC chemokine with potent activity on activated t cells through selective high affinity binding to CXCR3. J Exp Med 1998;187:2009–2021.

54. Stoll G, Nieswandt B. Thrombo-inflammation in acute ischaemic stroke—implications for treatment. Nat Rev Neurol 2019;15:473–481.